The *Vitis vinifera* receptor VvLYK6 negatively regulates chitin-triggered immune responses and promotes fungal infections

Jérémy Villette[1], Tania Marzari[1], David Landry[2], Thibault Roudaire[1], Agnès Klinguer[1], Nathalie Leborgne-Castel[1], Céline Vicedo[2], Virginie Gasciolli[2], Cécile Pouzet[3], Benoît Lefebvre[2], Marie-Claire Héloir[1], Benoit Poinssot[1*]

[1] Université Bourgogne Europe, Institut Agro, INRAE, UMR Agroécologie, Dijon, France

[2] Laboratory of Plant-Microbe-Environment Interactions (LIPME), Université de Toulouse, INRAE, CNRS, Castanet-Tolosan 31326, France

[3] TRI-FRAIB Imaging Platform Facilities, Fédération de Recherche Agrobiosciences Interactions et Biodiversité, Université de Toulouse, CNRS, UPS, 31320 Castanet-Tolosan, France

✉Corresponding author: benoit.poinssot@inrae.fr

Keywords: ***Vitis vinifera,*** **MAMP, chitin hexamer, inhibition, plant immunity, fungal pathogens**

Abstract

Botrytis cinerea is recognized as one of the most damaging fungal pathogens affecting grapevine (*Vitis vinifera*), directly impacting both grape yield and wine quality. Identifying new genes involved in the interaction between *V. vinifera* and *B. cinerea* appears to be a promising strategy for enhancing grapevine resistance in future breeding programs.

During pathogen infection, plasma membrane-localized pattern recognition receptors (PRRs) are responsible for detecting conserved microbe-associated molecular patterns (MAMPs). Among PRRs, members of the LysM receptor-like kinase family are well known to mediate the recognition of fungal MAMPs and triggering plant immune signaling pathways. Interestingly, a novel member of this receptor family, named VvLYK6, was identified in grapevine as the most highly upregulated during *B. cinerea* infection.

To investigate the role of VvLYK6 in plant immunity, we conducted overexpression studies in *Arabidopsis thaliana* and grapevine cell suspensions. Overexpression of *VvLYK6* led to a reduction in chitin-induced MAPK activation, decreased expression of defense-related genes, reduced callose deposition, and increased plant susceptibility to fungal pathogens in *A. thaliana*.

Based on these findings, we conclude that VvLYK6 acts as a negatively regulator of chitin-triggered immune responses, suggesting its potential role as a susceptibility gene during fungal infections.

Introduction

Grapevine (*Vitis vinifera*) is continuously exposed to intense pest pressure, including viruses, insects, oomycetes such as downy mildew (*Plasmopara viticola*) and fungi such as powdery mildew (*Erysiphe necator*) or grey mold (*Botrytis cinerea*). The current strategy to mitigate the impact of these diseases relies heavily on chemical treatments. However, these treatments pose risks to both the environment and human health, prompting the development of alternative approaches to disease management in vineyards (Pathak et al., 2022). One such approach involves the identification of resistance (*R*) and susceptibility (*S*) genes (Qiu et al., 2015; Zaidi et al., 2018). The introgression of *R* genes into grapevine has been a key strategy for developing durable disease-resistant varieties (Xiao et al., 2023). Notably, two members of the TIR-NB-LRR gene family from *Muscadinia rotundifolia* (a close related species of *V. vinifera*) have been identified as major *R* genes, conferring resistance to several important grapevine pathogens (Feechan et al., 2013). Interestingly, it has also been frequently observed that the loss of function of *S* genes can lead to broad-spectrum resistance, making them attractive targets for breeding programs (Zaidi et al., 2018).

Another promising strategy involves triggering grapevine immunity by eliciting plant defense responses with bioproducts (Adrian et al., 2024). Plant innate immunity relies on two well-characterized defense signaling pathways (Boller and Felix 2009). The first one is microbe-associated molecular pattern (MAMP)-triggered immunity (MTI), also referred to as pattern-triggered immunity (PTI). The second is the effector-triggered immunity (ETI) which is activated upon recognition of pathogen-derived effectors by plant resistance proteins (Böhm et al., 2014; Zipfel 2014). MTI represents the initial layer of plant immune defense, involving the recognition of conserved MAMPs released by invading microbes. These molecular patterns are detected by cell-surface pattern recognition receptors (PRRs), which initiate intracellular signal transduction cascades. This signaling typically involves phosphorylation events mediated by mitogen-activated protein kinases (MAPKs), ultimately leading to the activation of transcription factors and the expression of defense-related genes. Depending on the nature and concentration of the MAMPs, various defense responses can be triggered, including callose deposition, production of phytoalexins (such as stilbenes in grapevine), and synthesis of pathogenesis-related (PR) proteins (Ahuja et al., 2012; Zhou and Zhang, 2020).

Plant PRRs are structurally diverse and encompass several protein families, classified based on the nature of their extracellular domains (Ngou et al., 2022). Among these, the Lysin motif receptor-like kinases (LysM-RLKs) and Lysin motif receptor-like proteins (LysM-RLPs) are well-characterized for their ability to perceive various polysaccharides, including chitooligosaccharides (COS),

66 lipochitooligosaccharides (LCOs), and peptidoglycan (PGN). In all plant species, the LysM-RLK
67 family is subdivided into two main groups: LYK receptors, which possess an active kinase domain
68 capable of transducing signals into the cell, and LYR receptors, which contain an inactive kinase
69 domain and are presumed to act as co-receptors. In contrast, LysM-RLPs (also referred to as LYMs)
70 lack a kinase domain altogether and are thought to function in ligand recognition without direct signal
71 transduction (Buendia et al., 2018).
72 Chitin, a major structural component of fungal cell walls, is perceived by a complex of LysM-RLKs
73 and LysM-RLPs at the plasma membrane, which together mediate signal transduction. In *Arabidopsis*
74 *thaliana*, the LYR-type receptor AtLYK5, known for its high affinity for chitin oligomers, forms
75 heterodimers with another LYR receptor, AtLYK4 (Wan et al., 2012; Cao et al., 2014; Xue et al.,
76 2019). Despite their ability to bind chitin, the AtLYK4/5 complex cannot initiate intracellular signaling
77 due to their inactive kinase domains. Instead, signal transduction relies on the recruitment of the LYK-
78 type receptor AtCERK1, which possesses an active kinase domain but has relatively low affinity for
79 chitin oligomers (Miya et al., 2007; Cao et al., 2014). In rice (*Oryza sativa*), the LYK-type receptor
80 OsCERK1 plays a dual role in both immune and symbiotic signaling pathways (Zhang et al., 2021).
81 For immune responses, OsCERK1 interacts with LysM-RLPs such as OsCEBiP, OsLYP4, and
82 OsLYP6 to activate defense signaling upon chitin recognition (Shimizu et al., 2010; Ao et al., 2014).
83 In contrast, during the establishment of arbuscular mycorrhizal (AM) symbiosis, OsCERK1 forms a
84 complex with the LYR-type receptor OsMYR1 to mediate symbiotic signaling (He et al., 2019). These
85 studies collectively highlight the central role of OsCERK1 in signal transduction, functioning across
86 distinct biological contexts. The specificity of the signaling pathway depends on the nature of the ligand
87 and the high-affinity interaction with its corresponding receptor.
88 Phylogenetic analyses have revealed well-conserved clades within the LysM receptor family, reflecting
89 their functional specialization (Buendia et al., 2018). For example, the LYRIII C clade includes
90 AtLYK5 and MtLYR4, which share a conserved function in the perception of chitin oligomers and
91 play a role in MTI activation in *A. thaliana* and *Medicago truncatula*, respectively (Cao et al., 2014;
92 Feng et al., 2019). Similarly, the LYRI A clade, which comprises OsMYR1 and SlLYK10, is
93 functionally conserved in the perception of lipochitooligosaccharides (LCOs) and is involved in the
94 establishment of AM symbiosis in rice and tomato, respectively (Buendia et al., 2016; Girardin et al.,
95 2019; He et al., 2019; Cullimore et al., 2023). In grapevine, recent studies support a similar model in
96 which VvLYK1-1 and VvLYK1-2 (orthologs of AtCERK1), along with VvLYK5-1 (ortholog of
97 AtLYK5), mediate chitin signaling. These LysM-RLKs have been shown to participate in chitin
98 perception and restore MAPK activation, defense gene expression, and pathogen resistance in *A.*

99 *thaliana* mutants lacking functional chitin receptors (Brulé et al., 2019; Roudaire et al., 2023).
100 Moreover, the formation of a receptor complex between VvLYK1-1 and VvLYK5-1 was found to be
101 dependent on the presence of chitin oligomers. Interestingly, in grapevine, 16 LysM-RLK members
102 have been identified and classified into ten of the eleven phylogenetic clades defined by Buendia et al.
103 (2018), suggesting a broad diversification and potential functional specialization of this receptor family
104 in this species.
105 In the present study, we investigated the role of VvLYK6, a member of the *V. vinifera* LYRI B LysM-
106 RLK clade, which remains poorly characterized. Orthologs of VvLYK6 in various monocot and dicot
107 species, including tomato, have been implicated in the establishment of AM symbiosis (Li et al., 2022;
108 Ding et al., 2025). Interestingly, Brulé et al. (2019) reported that VvLYK6 was the most highly
109 expressed LysM-RLK during *B. cinerea* infection in susceptible mature grape berries. Using functional
110 genomics approaches, we demonstrated that VvLYK6 suppresses chitin-triggered immune responses
111 and increases plant susceptibility to three distinct fungal pathogens. Our findings suggest that VvLYK6
112 acts as a negative regulator of plant immunity, contributing to the heightened susceptibility to grey
113 mold. Therefore, *VvLYK6* may be considered as a novel *S* gene encoding a negative regulator of *V.*
114 *vinifera* immune responses.
115

116 **Materials and methods**

117 ***Plant materials and growth conditions***

118 *A. thaliana* wild-type (WT) Columbia (Col-0) ecotype, *Atcerk1* mutant (GABI-Kat_096F09, allele
119 *Atcerk1-2*; Gimenez-Ibanez et al., 2009) or transgenic lines Col-0-*p35S::VvLYK6*, Col-0-
120 *p35S::VvLYK6-GFP*, and *Atcerk1-p35S::VvLYK6* were grown under a 10/14-h day/night cycle at
121 20/18°C. Transgenic lines were obtained by floral-dip transformation (Clough and Bent, 1998) of the
122 Col-0 ecotype and *Atcerk1* mutant lines with coding sequence of *VvLYK6* (Vitvi05g00623) amplified
123 from complementary DNA (cDNA) of the susceptible *Vitis vinifera* cv. Marselan leaves and cloned
124 into the pFAST_R02 and pFAST_R05 (Shimada et al., 2010). Transgenic seeds were selected with
125 glufosinate (50 mg/L) and kanamycin (50 mg/L) selection for pFAST_R02 and pFAST_R05,
126 respectively, and subsequently genotyped (Figure S1). All experiments on *A. thaliana* were performed
127 on the third selected homozygous lines.
128 *V. vinifera* cv. Marselan cells were cultivated in Nitsch-Nitsch (NN) medium as detailed in Roudaire
129 et al. (2023). For experimentations, seven-day-old cultures were diluted twice with new medium.
130 Grapevine cells were transformed by co-cultivation with *Agrobacterium tumefaciens* culture with an

131 absorbance of 0.3 during 2 days. Then, cells were transferred in NN medium with agar (0.7 %)
132 supplemented with 250 mg/L cefotaxime and 50 mg/L kanamycin for selection. After 1 month, two
133 independent lines expressing *35S-VvLYK6-GFP* were selected.

134

135 ***Analysis of VvLYK6 gene expression in developmental and pathogen-infected grapevine tissues***

136 Microarray and data analysis were performed as described in Kelloniemi et al. (2015) from
137 grapevine (*V. vinifera cv. Marselan)* leaves and berries infected with *B. cinerea* and leaves infected
138 by *P. viticola*. *VvLYK6* expression profile of *V. vinifera* cv. Garganega berries infected with or
139 without *B. cinerea* was obtained from supplemental data of Lovato et al. (2019). Transcriptomic
140 data highlighting differential *VvLYK6* expression profile between pre-egression and egression
141 state in *V. vinifera* cv. Pinot Noir infected with *B. cinerea* were obtained from Haile et al. (2020).

142

143 ***Phylogenetic analysis of the VvLYKs***

144 Protein sequences for LysM-RLK family were retrieved using BLAST searches, in which A.
145 thaliana family members were used as query sequences against protein sequences from plant
146 species detailed in Table S1. A 1000 bootstrapped phylogenetic tree gathering 96 protein
147 sequences (Table S1) have been constructed with the Maximum Likelihood method and JTT
148 model (Jones et al., 1992). Alignment and phylogenetic analysis were performed with MEGA X
149 software (Kumar et al., 2018).

150

151 ***Pathogen assays***

152 The *B. cinerea* inoculum was produced by growing the strain BMM on solid medium (V8/2 tomato
153 juice, 1 % agar) in the dark to promote sporulation (Zimmerli et al., 2001). Conidia were isolated and
154 concentrated in water to infect *A. thaliana* leaves with a final concentration of $5x10^4$ conidia/mL diluted
155 in potato dextrose broth medium (PDB, 0.6%). Four-week-old Arabidopsis leaves were cut and placed
156 in survival conditions during *B. cinerea* infection. The *A. brassicicola* inoculum strain MIAE01824
157 originated from Agroecology unit collection (UMR1347, Dijon, France) was grown 20 days on solid
158 potato dextrose agar medium (PDA, 19 $g.L^{-1}$) supplemented with sucrose (20 $g.L^{-1}$) and $CaCO_3$ (30
159 $g.L^{-1}$) at 20°C in the dark. Four-week-old Arabidopsis leaves were cut and placed in survival conditions

160 during *A. brassicicola* infection. Lesion surfaces caused by these two necrotrophic fungi were
161 measured with imageJ software (https://imagej.net/ij/).
162 *Erysiphe necator* assays were performed as described by Roudaire et al. (2023). Fungal structures were
163 visualized using a Leica DMA light microscope (magnification x400). For each treatment, 100
164 germinated spores were evaluated. The percentage of successful epidermal cell penetration was
165 determined based on the presence of a haustorium within the cell or the emergence of secondary hyphae
166 from the appressorium, as previously described by Roudaire et al. (2023). Three biological independent
167 experiments were performed.

168

169 ***Confocal microscopy***

170 Confocal microscopy was performed using a Leica TCS SP8 multiphoton microscope with a 40X oil-
171 immersion objective. Marselan suspension cells and leaf segments of *A. thaliana* lines expressing
172 *VvLYK6* tagged with GFP were mounted directly or in ultrapure water between slide and coverslips,
173 respectively and observed. For plasma membrane staining, samples were incubated in 10 µM FM4-64
174 during 10 min prior to observation. Fluorescent markers were excited with the 488 nm laser. GFP and
175 FM4-64 emissions were bandpass filtered at 500-525 nm and between 616 - 694 nm, respectively.
176 Pictures were then treated with LAS X software.

177

178 ***Elicitors and plant treatment***

179 In this study, we used as elicitors a purified hexamer (DP6) of chitin (GLU436, Elicityl, Crolles, France
180 at a concentration of 0.05 g/L) and flg22 peptide from *X. campestris* pv. campestris strain 305
181 (QRLSSGLRINSAKDDAAGLAIS) at 10^{-6} or 10^{-8} M, depending on the bioassay (Trdá et al., 2014).
182 For *A. thaliana* treatments, four-weeks old plant leaves were pre-infiltrated with ultrapure water and
183 placed on 6-wells plate containing ultrapure water during 4 h. Then, ultrapure water was replaced by
184 either ultrapure water (control) or elicitors in contact with leaves during 10 min for MAPKs activation
185 and one hour for RT-qPCR experiments before freezing samples in liquid nitrogen.
186 Grapevine cell suspensions were equilibrated at 0.1 g/mL and shacked under the same conditions as
187 for their culture. Treatment was done in a volume of 20 mL with a final concentration of 0.05 g/L chitin
188 DP6, cells were harvested in liquid nitrogen at 10 min post-treatment for MAPKs activation and 1hour
189 post-treatment for RT-qPCR analysis.

190

191 ***MAPKs phosphorylation***

192 For MAPK phosphorylation, treated *A. thaliana* leaves or grapevine cells were crushed in liquid
193 nitrogen and total proteins were extracted with a solution containing 50mM HEPES (pH 7.5), 5mM
194 EGTA (pH 8.1), 5 mM EDTA, 1mM Na_3VO_4, 50 mM β-glycerophosphate, 10 mM NaF, 1 mM de
195 phenylmethanesulfonyl fluoride, 5 mM dithiothreitol and complete EDTA-free protease inhibitor
196 cocktail (Roche). Phosphorylation of MAPKs was detected by immunoblotting of 25µg total proteins
197 using an anti-p42/44-phospho-ERK antibody (Cell Signaling Technology). Antibody was then
198 revealed using ECL prime (Cytiva) western blotting detection reagent with an Amersham
199 ImageQuant800 (Cytiva). Quantification of MAPKs intensity was normalized by total proteins stained
200 by Ponceau red with the ImageQuant software.

201

202 ***Real-time quantitative PCR (RT-qPCR) analysis***

203 For RT-qPCR experiments, treated leaves or cells were crushed in liquid nitrogen and total RNA was
204 extracted with the SV Total RNA Isolation System with DNAse treatment (Promega). First-strand
205 cDNAs were synthesized with the High-Capacity cDNA Reverse Transcription kit (Applied
206 Biosystems). RT-qPCR was performed in a ViiA™ 7 Real-Time PCR system (Applied Biosystems)
207 with 10 ng cDNA and 1X GoTaq® qPCR Master Mix (Promega). Relative gene expression was
208 assessed taking into consideration the efficiency (E) of each reaction calculated by the LinRegPCR
209 quantitative PCR data analysis program (Ruijter et al., 2009). Gene expression values were normalized
210 with two housekeeping genes corresponding to *AtRHIP1* (At4g26410) and *AtPTB1* (At3g01150) for
211 RT-qPCR experiments on *A. thaliana* and *VvRPL18B* (Vitvi05g00033) and *VvVPS54* (Vitvi10g01135)
212 for RT-qPCR assays on grapevine cells (*Vitis vinifera* cv. Marselan). All primers used are listed in
213 Table S2.

214

215 ***Callose deposition analysis***

216 Four-week-old Arabidopsis were sprayed on both sides with either water (as control) or chitin DP6
217 (0.05 g/L). Four days post-treatment, two leaves of three independent plants per condition were
218 sampled and fixed in absolute ethanol during one night. The aniline blue staining was performed as
219 detailed in Roudaire et al. (2023). Leaves were then observed on adaxial side by epifluorescence
220 microscopy under λex = 340-380 nm and λem = 425 nm, magnification x100, Leica DMRB. Callose
221 deposits were acquired for each condition using the Nis Elements BR software (Nikon) with the DS-

222 5Mc-U1 digital photomicrographic camera (Nikon). Image analysis was then performed on the Fiji
223 application as described in Mason et al. (2020) with Trainable Weka Segmentation plugin.

224

225 **Transient expression for FRET-*FLIM analysis***

226 The transient expression in *Nicotiana benthamiana* leaves were previously described in Girardin et al.
227 (2019) using Agrobacteria containing a cassette overexpressing either VvLYK1-1^{G328E} (Brulé et al.,
228 2019) fused with a C-terminal Cyan Fluorescent Protein (CFP) alone or with VvLYK6 or VvLYK5-1
229 (Roudaire et al., 2023) tagged with a C-terminal Yellow Fluorescent Protein (YFP) (Karimi et al.,
230 2005). The kinase-dead mutant version of VvLYK1-1 (VvLYK1-1^{G328E}) was generated using the Quik
231 Change Site-Directed Mutagenesis protocol (Liu and Naismith, 2008). FLIM was performed on an
232 inverted LEICA DMi8 microscope equipped with a TCSPC system from PicoQuant. The excitation of
233 the CFP donor at 440 nm was carried out by a picosecond pulsed diode laser at a repetition rate of 40
234 MHz, through an oil immersion objective (63×, N.A. 1.4). The emitted light was detected by a Leica
235 HyD detector in the 450-500 nm emission range. Images were acquired with acquisition photons of up
236 to 1500 per pixel. Data were acquired in 3 independent experiments and pooled. From the fluorescence
237 intensity images, the decay curves of CFP were calculated per pixel and fitted (by Poissonian maximum
238 likelihood estimation) with either a double- or tri-exponential decay model using the SymphoTime 64
239 software (PicoQuant, Germany). The double-exponential model function was applied for donor
240 samples with only CFP present. The tri-exponential model function was used for samples containing
241 CFP and YFP.

242

243 ***Co-immunopurification with VvLYK1-1***

244 For co-immunopurification, the sequence coding VvLYK1-1^{G328E} was fused to the sequence coding
245 a triple hemaglutin (HA) tag. VvLYK1-1^{G328E}-HA and VvLYK6-YFP or VvLYK5-1-YFP were
246 expressed into *N. benthamiana*. Leaf material was collected 3 days after infiltration and co-
247 immunopurification was performed as described in Ding et al. (2024), except that anti-HA beads
248 (pierce Anti-HA magnetic beads, 88836) were used for purification and anti-HA-HRP antibodies
249 (Roche, Anti-HA-Peroxidase High affinity from rat IgG1, 12013819001) were used for Western-
250 blotting. Chitin DP6 (CO6) at 0.1 g/L was infiltrated into leaves before harvest and added in the IP
251 buffer for protein solubilisation and wash of the beads.

252

253 **Microsomal fraction preparation and binding assay**

254 Preparation of microsomal fraction, and binding assays were previously described in Girardin et al.,
255 2019. CO5-biotin and CO7-biotin were synthesized as detailed in Cullimore et al., 2023. Briefly,
256 binding assays with CO5-biotin and CO7-biotin were conducted on microsomal fractions in binding
257 buffer described in Girardin et al. (2019) for 1h at 4 °C. For western-blotting, proteins were separated
258 by SDS-PAGE using homemade 6 % polyacrylamide gels and transferred onto a nitrocellulose
259 membrane with a transblot system (Bio-rad). The membranes were blocked for 1h and incubated for
260 1h with the following antibodies: αGFP (11814460001, Roche, 1:3000), and then goat αMouse-HRP
261 (1706516, Bio-Rad, 1:10000) or streptavidin-HRP (S911, Invitrogen, 1:3000). The chemiluminescent
262 signal from HRP was observed using Chemidoc system (Bio-Rad).

263

264 **Results**

265 ***Analysis of VvLYK6 expression suggests an important role during B. cinerea infection***

266 To investigate the role of VvLYK6 in grapevine immunity, we examined its expression profile using
267 our previously published transcriptomic dataset (Kelloniemi et al., 2015). Our analysis revealed that
268 *VvLYK6* is upregulated in susceptible *V. vinifera* leaves at 24 and 48h post-infection (hpi) with *B.*
269 *cinerea*, whereas its expression remains unchanged following infection with *P. viticola* (Figure 1A).
270 Given that VvLYK6 belongs to the LysM-RLK family known to perceive COS, these results are
271 consistent with the presence of chitin in the fungal cell wall of *B. cinerea*, which is nearly absent in
272 that of the oomycete *P. viticola*. However, *VvLYK6* expression was not significantly induced in
273 grapevine cells treated with chitin hexamers (Figure S2A). We also observed that *VvLYK6* expression
274 is induced after 48h of *B. cinerea* infection on grapevine fruits (Figure 1B) and particularly in infected
275 mature berries (Figure 1C) which are known to be very susceptible to grey mold (Kelloniemi et al.,
276 2015). To corroborate these results and confirm the upregulation of *VvLYK6* during *B. cinerea*
277 infection, we analyzed other publicly available transcriptomic data (Figure S2B-C). In a first study on
278 mature berries of the susceptible *V. vinifera* cv. Garganega inoculated or not with *B. cinerea*, *VvLYK6*
279 expression was significantly increased in infected berries compared to uninfected ones twelve days
280 post-inoculation (Lovato et al., 2019, Figure S2B). In a second study comparing ripe berries of the
281 susceptible *V. vinifera* cv. Pinot Noir with and without visible symptoms of *B. cinerea* infection
282 (referred to as egression and pre-egression, respectively), the expression of *VvLYK6* was significantly
283 upregulated only in berries displaying visible symptoms (Haile et al., 2020, Figure S2C). All together,

284 these results showed a correlation between *VvLYK6* upregulation in mature grapevine berries and their
285 high susceptibility to *B. cinerea*.

286

287 ***VvLYK6 belongs to the LYRI B clade with conserved domain of LysM-receptor like kinase***

288 To investigate the function of VvLYK6, we first conducted a phylogenetic analysis involving several
289 plant species known to possess well-characterized LysM-RLKs associated with immunity and/or
290 symbiosis. LysM-RLK protein sequences were retrieved from *A. thaliana*, *Hordeum vulgare, Oryza*
291 *sativa*, *Medicago truncatula*, *Musa acuminata*, *Prunus persica*, *Solanum lycopersicum* and *V. vinifera*
292 (Supplementary Table S1). A total of 96 protein sequences were selected to construct a maximum-
293 likelihood phylogenetic tree (Figure 2A). The resulting tree displays the two well-known sub-groups
294 (LYKs and LYRs) further divided in eleven clades as described by Buendia et al. (2018). The 16
295 members of the LysM-RLK family in *V. vinifera* are distributed across all clades except for the LYKIV
296 clade, which is not conserved among dicots (Figure 2A). Our study focused on VvLYK6 (indicated by
297 a black arrow), which belongs to the LYRI B clade, a group whose function has never yet been
298 characterized in *V. vinifera*.

299 We began by analyzing the putative structure of VvLYK6, confirming the presence of all conserved
300 domains typical of LysM-RLKs: a signal peptide, three extracellular LysM domains, a transmembrane
301 domain, and a cytoplasmic putative serine/threonine kinase domain (Figure 2B, Table S3). Regarding
302 the intracellular kinase domain, most of the amino acids of the kinase domain present in LYKI
303 members (e.g. AtCERK1, VvLYK1-1, VvLYK1-2) were conserved in LYRI B orthologs, including
304 VvLYK6 (Figure 2B). However, deletions observed in the glycine-rich loop, along with the lack of
305 conservation in the catalytic loop and activation segment (both essential for kinase activity) suggest
306 that the kinase domain of VvLYK6, as well as other members of the LYRI B may be catalytically
307 inactive (Hanks et al., 1988; Klaus-Heisen et al., 2011). Specifically, while the glycine-rich loop
308 typically contains three to four conserved glycine residues in most LYK subgroup members with kinase
309 activity, only a single glycine residue is present in LYRI B members. Furthermore, other key motifs
310 associated with kinase function, such as the catalytic loop (RD) and the activation segment (DFG),
311 which are well conserved in active LYK kinases, are absent in the LYRI B clade (Figure 2B).

312 To determine the subcellular localization of VvLYK6, we expressed a C-terminal GFP-tagged version
313 of the protein in *A. thaliana* and *V. vinifera*. Transgenic lines exhibited green fluorescence from
314 VvLYK6-GFP which co-localized with the red fluorescence of the plasma membrane marker FM4-64
315 (Brandizzi et al., 2004) in both plant species (Figure 2C, Figure S3). Plasmolysis experiments further

316 confirmed that VvLYK6 followed the plasma membrane during cell shrinkage (Figure 2C) supporting
317 its predicted localization at the plasma membrane.

318

319 ***Constitutive expression of VvLYK6 in A. thaliana increases its susceptibility to B. cinerea and***
320 ***other adapted or non-adapted fungal pathogens***

321 To investigate the role of VvLYK6 during *B. cinerea* infection, and taking advantage of the fact that
322 *VvLYK6* has no ortholog in *A. thaliana*, we constitutively expressed its gene from the susceptible *V.*
323 *vinifera* cv. Marselan under the control of the *CaMV35S* promoter (*p35S*) in the wild-type (WT)
324 ecotype Col-0 of *A. thaliana*. Three independent lines exhibiting high levels of *VvLYK6* transcripts
325 were selected (Figure S4A). To assess the impact of *VvLYK6* expression during fungal infections,
326 leaves were inoculated with *B. cinerea* and lesion areas were quantified three days post-inoculation
327 (dpi). As shown in Figure 3A and Figure S4B, all three transgenic lines displayed a significant increase
328 in susceptibility to *B. cinerea*, with lesion areas approximately 50% larger than those observed in WT
329 plants.
330 We next examined whether VvLYK6 expression influenced susceptibility to other fungal pathogens.
331 First, we tested the necrotrophic fungus *Alternaria brassicicola*, which is adapted to Brassicaceae. At
332 5 dpi, the three transgenic lines showed significantly larger lesion areas, ranging from 26% to 67%,
333 compared to WT plants (Figure 3B, Figure S4C).
334 Finally, we evaluated the response to the non-adapted biotrophic fungus *Erysiphe necator* (grapevine
335 powdery mildew). The Arabidopsis transgenic lines expressing *VvLYK6* exhibited a significantly
336 higher rate of epidermal cell penetration compared to WT plants, with approximately 50% of cells
337 penetrated in transgenic lines versus 30% in controls (Figure 3C).
338 All these results suggest that VvLYK6 may interfere with plant immune responses, thereby facilitating
339 fungal colonization and spread.

340

341 ***Constitutive expression of VvLYK6 inhibits chitin-triggered immune responses in A. thaliana***

342 To further elucidate the function of VvLYK6, we investigated early defense responses triggered by
343 chitin by analyzing MAPK phosphorylation levels. As previously reported (Roudaire et al., 2023),
344 chitin oligomers induce transient phosphorylation of two mitogen-activated protein kinases (MAPKs)
345 of 43 and 47 kDa in *A. thaliana* WT plants (Figure 4A), corresponding to MPK3 and MPK6,
346 respectively (Claverie et al., 2018). Interestingly, phosphorylation of both MAPKs, measured 10 min

347 after treatment with chitin hexamers (DP6), was significantly reduced, by approximately 40%, in all
348 three independent *VvLYK6*-expressing lines compared to WT plants (Figure 4A–B). To rule out a
349 delayed activation of MAPKs in transgenic lines, phosphorylation levels were also assessed 20 min
350 post-treatment, but no compensatory increase was observed (Figure 4A).
351 In addition, we examined the expression of two defense-related genes: *AtFRK1* (flagellin-induced
352 receptor kinase 1) and *AtRBOHD* (respiratory burst oxidase homolog D), both known to be induced by
353 chitin DP6 treatment (Morales et al., 2016; Brulé et al., 2019). Expression of *AtFRK1* was significantly
354 reduced in the three transgenic lines, with transcript levels decreased by 56% to 71% compared to WT
355 (Figure 4C). Similarly, *AtRBOHD* transcript levels were reduced by 67% to 74% in the *VvLYK6*-
356 expressing lines (Figure 4D). To further explore the function of VvLYK6**,** we analyzed additional
357 immune-related genes involved in hormonal signaling pathways, such as salicylic acid (SA) and
358 jasmonic acid (JA) (Spoel et al., 2003). No significant differences were observed in the expression of
359 the SA- and JA-responsive genes *PR1* and *PDF1.2* between the three independent *VvLYK6*-expressing
360 lines and WT plants following chitin DP6 treatment (Figure S5).
361 We then examined the impact of VvLYK6 expression on callose deposition, a later-stage defense
362 response. Chitin is well known to induce callose accumulation in *A. thaliana* leaves (Roudaire et al.,
363 2023). Compared to WT plants, all transgenic lines expressing *VvLYK6* exhibited a significantly
364 reduced percentage of callose deposits four days after chitin DP6 treatment (Figure 4E–F). Specifically,
365 WT leaves showed callose deposits covering 0.2% of the total leaf area, whereas the transgenic lines
366 averaged only 0.04%, a level comparable to water-treated controls (Figure 4E–F).
367 Taken together, these results clearly indicate that VvLYK6 expression in *A. thaliana* suppresses chitin-
368 triggered immune responses.
369 Although our study primarily focused on the role of VvLYK6 during fungal infection and chitin
370 perception, given its induction during *B. cinerea* infection, we also tested its specificity by analyzing
371 responses to a bacterial MAMP: the flagellin-derived peptide flg22 (Trdá et al., 2014). MAPK
372 phosphorylation was assessed 10 min after flg22 treatment in WT and *VvLYK6*-expressing lines.
373 Immunoblot analysis revealed no significant differences between the transgenic lines and WT (Figure
374 S6A). As flg22 is also known to inhibit plant growth in *A. thaliana* (Vetter et al., 2012), flg22-induced
375 growth inhibition assays were performed. After 12 days of growth on a medium containing 1 µM flg22,
376 no significant differences in growth inhibition were observed between WT and *VvLYK6*-expressing
377 seedlings (Figure S6B).

378 These findings demonstrate that VvLYK6 expression in *A. thaliana* does not interfere with flg22-
379 triggered immune signaling, but appears to specifically modulate chitin-induced immune responses
380 associated with fungal pathogens.

381

382 ***VvLYK6 represses chitin-triggered immunity in grapevine (Vitis vinifera)***

383 To validate the findings observed in *A. thaliana*, we investigated the function of VvLYK6 in *V.*
384 *vinifera*. Two independent grapevine cell lines constitutively expressing VvLYK6 tagged with GFP
385 and exhibiting high transcript and protein levels were selected (Figure S7A–B).
386 Chitin oligomers are known to elicit phosphorylation of two MAPKs (45 and 49 kDa) in grapevine
387 cells (Brulé et al., 2019). Compared to WT cells, MAPK phosphorylation induced by chitin DP6 was
388 significantly reduced by 25% to 35% in both transgenic lines (*VvLYK6* OE#1 and OE#2) after 10 min
389 of treatment (Figure 5A, Figure S7C). We also quantified the expression of two defense-related genes
390 involved in the stilbene biosynthetic pathway, which contributes to phytoalexin production in
391 grapevine: *VvPAL* (phenylalanine ammonia lyase) and *VvSTS1.2* (stilbene synthase). One hour after
392 chitin DP6 treatment, the constitutive expression of *VvLYK6* significantly impaired the induction of
393 both genes. The typical upregulation of *VvPAL* and *VvSTS1.2* was reduced by more than 50% in the
394 transgenic lines compared to WT cells (Figure 5B–C). On the whole, these results suggest that
395 VvLYK6 acts as a negative regulator of chitin-triggered immune responses in *V. vinifera*, consistent
396 with the observations made in *A. thaliana*.

397

398 **VvLYK6 forms a receptor complex with VvLYK1-1 in presence of chitin oligomers**

399 During fungal infection or in the presence of chitin, VvLYK1-1 has been identified as a key co-receptor
400 involved in chitin-triggered immune signaling in grapevine (Brulé et al., 2019). Notably, VvLYK1-1
401 is the only LysM-RLK shown to form a receptor complex with VvLYK5-1 to perceive chitin and
402 activate downstream defense responses (Roudaire et al., 2023).
403 To explain the repression of microbe-triggered immunity (MTI) observed when *VvLYK6* is
404 overexpressed, we hypothesized a potential interaction between the functional co-receptor VvLYK1-1
405 and VvLYK6**.** To test this, we performed FRET-FLIM experiments following transient co-expression
406 of both proteins fused to CFP and YFP, respectively. Since constitutive expression of VvLYK1-1
407 induces strong cell death in *Nicotiana benthamiana*, we used a kinase-dead version carrying the G328E
408 mutation (VvLYK1-1^{G328E}-CFP). As expected, the CFP lifetime of VvLYK1-1^{G328E}-CFP expressed

409 alone was unaffected by chitin treatment (Figure 6A). However, co-expression with VvLYK6-YFP
410 followed by chitin DP6 treatment resulted in a significant decrease in CFP lifetime, indicating a ligand-
411 dependent *in vivo* interaction between these two LysM-RLKs (Figure 6A). This interaction was further
412 confirmed by co-immunoprecipitation (Co-IP) assays, which demonstrated that VvLYK6-YFP
413 physically associates with VvLYK1-1^{G328E}-HA in the presence of chitin DP6 (Figure 6B). In both
414 experiments, VvLYK5-1 was used as a positive control, as its interaction with VvLYK1-1 in a ligand-
415 dependent manner has been previously described (Figure 6A–B; Roudaire et al., 2023). Interestingly,
416 VvLYK6 and VvLYK1-1 primarily interact in the presence of chitin DP6, suggesting that VvLYK6
417 may possess affinity for chitin oligomers. Indeed, some LYRI B orthologs have been reported to bind
418 both short- and long-chain chitin oligomers with high affinity (Li et al., 2022; Ding et al., 2025). To
419 evaluate the binding capacity of VvLYK6, we used cross-linkable biotinylated versions of chitin
420 pentamer and heptamer (CO5-biotin and CO7-biotin) to assess its interaction with chitin oligomers.
421 Surprisingly, unlike its orthologs in *Brachypodium distachyon* (BdLYR2) and *Medicago truncatula*
422 (MtLYR8), VvLYK6 did not exhibit high-affinity binding to either CO5 or CO7 (Figure 6C; Li et al.,
423 2022; Ding et al., 2025). This discrepancy may be due to improper folding of VvLYK6 when
424 overexpressed in *Nicotiana benthamiana* leaves, resulting in a non-functional protein. Alternatively,
425 VvLYK6 may require association with VvLYK1-1 to properly bind chitin oligomers and initiate signal
426 transduction. Supporting this last hypothesis, constitutive expression of VvLYK6 in the *Arabidopsis*
427 mutant *Atcerk1* failed to activate MAPK phosphorylation or induce *FRK1* expression following chitin
428 DP6 treatment (Figure S8). These findings suggest that VvLYK6 may not function as a primary chitin
429 receptor but could act as a modulator of immune signaling through interaction with VvLYK1-1.

430

431 **Discussion**

432 *B. cinerea* is among the most devastating fungal pathogens affecting a wide range of plant species.
433 This necrotrophic fungus is particularly known for infecting mature berries of susceptible *V. vinifera*
434 cultivars, leading to significant reductions in yield and must quality during winemaking (Fillinger and
435 Elad, 2016). Numerous transcriptomic studies have highlighted the upregulation of specific genes
436 during berry ripening, a developmental stage highly susceptible to infection (Kelloniemi et al., 2015;
437 Lovato et al., 2019; Haile et al., 2020).
438 Chitin, a major structural component of fungal cell walls, is recognized as a MAMP. In the context of
439 *B. cinerea* infection, we focused on the well-characterized LysM-RLK family, which plays a key role

440 in the in the perception of chitin oligomers and the activation of immune responses. In susceptible *V.*
441 *vinifera* varieties, *VvLYK6* has been identified as the most highly expressed LysM-RLK during *B.*
442 *cinerea* infection in mature berries (Kelloniemi et al., 2015; Brulé et al., 2019), a finding further
443 supported by additional transcriptomic analyses (Lovato et al., 2019; Haile et al., 2020).
444 Our study provides new insights into the role of *VvLYK6*, a member of the newly defined LYRI B
445 subfamily. Unexpectedly, we found that the constitutive expression of *VvLYK6* in *A. thaliana*
446 significantly increases the plant susceptibility to *B. cinerea* and two other adapted and non-adapted
447 fungal pathogens. More specifically, our results indicate that the inhibitory function of *VvLYK6* is
448 confined to the chitin-triggered defense pathway associated with fungal pathogens.
449 In *V. vinifera*, the constitutive expression of *VvLYK6* similarly inhibits the chitin-triggered immune
450 pathway. Morevoer, VvLYK6 has been shown to form a heterodimeric complex with VvLYK1-1 in
451 the presence of chitin oligomers, suggesting potential competition between VvLYK6 and VvLYK5-1
452 for complex formation with VvLYK1-1 (Roudaire et al., 2023). During *B. cinerea* infection in mature
453 berries, the upregulation of *VvLYK6* may lead to a predominance of VvLYK1-1/VvLYK6 complexes,
454 especially since *VvLYK6* expression does not affect *VvLYK5-1* transcript levels (Figure S7D). This
455 could negatively regulate the formation of *VvLYK1-1/VvLYK5-1* complexes, supporting a model in
456 which *VvLYK6* expression modulates chitin-triggered immunity in grapevine (Figure 7). A similar
457 regulatory mechanism has been described in rice within the LysM-RLK family. The rice ortholog of
458 VvLYK1-1, OsCERK1, is known to participate in both immune responses, via interaction with
459 *OsCEBIP*, and AM symbiosis via interaction with OsMYR1. Notably, constitutive expression of
460 *OsMYR1*, a member of the LYRI A clade, significantly reduces disease resistance in rice (Zhang et al.,
461 2021). Analogous regulatory dynamics have also been observed in other RLK families. For instance,
462 the Leucine-Rich Repeat RLK *BIR2* acts as a negative regulator by forming a complex with *BAK1*,
463 thereby preventing *BAK1* from associating with ligand-binding receptors such as *FLS2* in the presence
464 of MAMPs (Halter et al., 2014).
465 During chitin-triggered immunity in *V. vinifera*, *VvLYK6* expression appears to be negatively
466 correlated with the expression of the well-established defense-related gene *VvPAL* and *VvSTS1.2*,
467 encoding the phenylalanine ammonia lyase and the stilbene synthase, respectively. These two enzymes
468 catalyze the final step in the biosynthesis of resveratrol, the main grapevine phytoalexin. When *VvLYK6*
469 is overexpressed in grapevine cells, the expression of *VvPAL* and *VvSTS1.2* is significantly suppressed.
470 These findings are consistent with the observed susceptibility of *V. vinifera* to *B. cinerea* during berry
471 ripening. While green berries typically exhibit basal resistance to *B. cinerea*, mature berries become
472 highly susceptible at harvest. At the veraison stage, Kelloniemi et al. (2015) showed that the defense-

473 related gene *VvPAL* and *VvSTS1.2* are significantly upregulated in green berries infected by *B. cinerea*,
474 leading to the accumulation of resveratrol, while the expression of *VvLYK6* remains very low. In
475 contrast, in mature berries, *VvLYK6* is strongly upregulated during infection, while *VvPAL* and
476 *VvSTS1.2* are not induced, resulting in increased susceptibility to the pathogen (Kelloniemi et al.,
477 2015). Our findings suggest that *VvLYK6* may act as a key molecular component influencing the
478 expression of *VvPAL* and *VvSTS1.2*, thereby modulating grapevine susceptibility to *B. cinerea*
479 infection. Interestingly, similar patterns have been observed in other species, such as tomato, where
480 ripe fruits are significantly more susceptible to *B. cinerea* than unripe ones (Silva et al., 2021). In that
481 study, transcriptomic analyses revealed an upregulation of *SlLYK9*, the tomato ortholog of *VvLYK6*
482 (Figure 1), in ripe fruits infected by the necrotrophic fungi *B. cinerea* and *Rhizopus stolonifer* (Figure
483 S9). As in grapevine, the upregulation of *SlLYK9* correlates with increased susceptibility in mature
484 tomato fruits, suggesting a conserved role in the suppression of plant defense responses (Silva et al.,
485 2021). These observations point to a broader functional role for LysM-RLKs belonging to the LYRI B
486 clade. While LYRI B members have traditionally been associated with the establishment of symbiosis
487 (Li et al., 2022; Ding et al., 2025), emerging evidence suggests they may also act as negative regulators
488 of plant immunity across different organs and plant–fungus interactions. This dual role is supported by
489 their expression in both root and aerial tissues (leaves and fruits) in grapevine and tomato (Figure S10).
490 Such functional versatility has also been reported for other LysM-RLK clades. Members of the LYRI A
491 clade, for example, are involved in symbiosis and can act as either positive or negative regulators of
492 immunity depending on the plant species (Buendia et al., 2018; Zhang et al., 2021), although their
493 expression is typically restricted to roots. Similarly, LYRIII C genes function as negative regulators of
494 both immunity and AM symbiosis and are expressed in both root and aerial tissues (Wang et al., 2023).
495 Taken together, these findings suggest that LYRI B members may serve as repressors of plant
496 immunity in aerial organs during *B. cinerea* infection, while also contributing to AM symbiosis in
497 roots. The potential role of *VvLYK6* in AM establishment warrants further investigation, particularly
498 since, unlike other LYRI B proteins, it does not appear to retain a high affinity for chitooligosaccharides
499 (COS).
500 From an evolutionary perspective, we analyzed the LYK6 receptor sequence from *Muscadinia*
501 *rotundifolia (*MrLYK6), a species closely related to *V. vinifera* and naturally resistant to *B. cinerea*
502 (Gabler et al., 2003). Sequence alignment between MrLYK6 and VvLYK6 revealed a high identity of
503 95.4%, with more than half of the amino acid variations located within the LysM2 domain (Figure
504 S11A). This domain has been shown to play a critical role in chitin binding in OsCEBIP, AtCERK1
505 and OsCERK1 with specific residues directly involved in ligand interaction (Liu et al.; 2012; Hayafune

506 et al., 2014; Xu et al., 2023). Notably, multiple sequence alignment revealed differences between
507 VvLYK6 and MrLYK6 at several key residues known to be essential for chitin binding in the
508 aforementioned receptors (Figure S11A–B). To further investigate these differences, we used
509 AlphaFold3 to predict the three-dimensional structures of the LysM2 domains of VvLYK6 and
510 MrLYK6, based on the crystallized structure of OsCERK1 bound to a chitin hexamer (Xu et al., 2023).
511 These structural models revealed distinct differences in both electrostatic charge distribution and
512 conformational features within the chitin-binding region (Figure S11C). Taken together, these natural
513 variations in the LysM2 domain of VvLYK6 may explain its lack of detectable affinity for chitin
514 oligomers when expressed alone (Figure 6C). Conversely, the putative chitin-binding capacity of
515 MrLYK6 could contribute to the enhanced resistance of *M. rotundifolia* to *B. cinerea*, highlighting the
516 evolutionary divergence of LysM-RLK function even among closely related species.
517 To conclude, our study demonstrates that VvLYK6 forms a chitin-induced receptor complex with
518 VvLYK1-1, and that its overexpression negatively regulates plant immune responses, thereby
519 enhancing susceptibility to *B. cinerea* and other fungal pathogens. These findings support the
520 classification of *VvLYK6*, particularly in susceptible *V. vinifera* cultivars, as a susceptibility (*S*) gene.
521 Consequently, targeted knock-out of *VvLYK6* represents a promising strategy to improve grapevine
522 resistance to *B. cinerea* and potentially other fungal pathogens. In line with the growing interest in *S*
523 genes as complementary or alternative targets to classical resistance (*R*) genes in crop improvement
524 (Zaidi et al., 2018), *VvLYK6* emerges as a compelling candidate for genome editing approaches.
525 Furthermore, we identified naturally occurring mutations between *LYK6* from *M. rotundifolia* and *V.*
526 *vinifera*, which may underlie differences in disease resistance. These beneficial allelic variants could
527 be harnessed through base editing technologies to precisely engineer enhanced resistance traits,
528 offering a novel and sustainable avenue for grapevine breeding.

529

530

531 **Conflict of interest**

532 The authors declare no potential conflict of interest.

533 **Author contributions**

534 JV performed the most of experiments and data analysis. JV, BL, MCH and BP designed the project,
535 experiments and wrote the article. JV produced all transgenic lines of *A. thaliana* excepts lines

536 expressing *VvLYK6* in Col-0 genetic background generated by TR. JV performed all experiments
537 carried out on *A. thaliana* described in this article. NLC and AK transformed and selected grapevine
538 cells for *VvLYK6* overexpression. TM performed all experiments on grapevine cells including
539 treatments and RT-qPCR, Western Blot were done by JV. DL performed transient expression of *VvLYK*
540 in tobacco, microsomal fractions, binding assays and FLIM experiments with CP. TM, CV and VG
541 performed co-IP experiment.

542 **Funding**

543 This work has been supported by Plant2Pro® Carnot Institute in the frame of its 2020 call for projects
544 (VitiLYKs project, grant #C4520) which is supported by the French National Research Agency (ANR
545 20-CARN-024-01) and the PPR VITAE (ANR 20-PCPA-0010).

546 **Acknowledgements**

547 We acknowledge Abdelwahad Echairi and Anna Beslic (SATT Sayens, Dijon, France) for the E.
548 necator strain. We also acknowledge Dr Christian Steinberg for the A. brassicicola inoculum strain
549 MIAE01824 originated from Agroecology unit collection (UMR1347, Dijon, France). We
550 acknowledge Cécile Blanchard for her technical support concerning the infection with the different
551 pathogens. *We acknowledge* Elodie Noirot for confocal microscopy supports from the regional Centre
552 of Microscopy/DImaCell platform (Dijon, France). *We also acknowledge France-BioImaging*
553 *infrastructure supported by the French National Research Agency (ANR-10-INBS-04).*

554 **Supplementary Material**

555 Supplementary Figures S1, S2, S3, S4, S5, S6, S7, S8, S9, S10 and S11 have been uploaded
556 separately in a pdf file.

557 Supplementary Tables S1, S2, S3 have been uploaded separately in a excel file.

558 **References**

559

560 Adrian M, Corio-Costet M-F, Calonnec A, Cluzet S, Poinssot B, Trouvelot S, Wiedemann-
561 Merdinoglu S, Viaud M (2024) Chapter Four - Grapevine defence mechanisms when
562 challenged by pathogenic fungi and oomycetes. In: Martins-Lopes P, ed. Advances in
563 Botanical Research. Grapevine: From Origin to the Vineyard. Academic Press, 101–195.

564 Ahuja I, Kissen R, Bones AM (2012) Phytoalexins in defense against pathogens. Trends in Plant
565 Science 17: 73–90

566 Ao Y, Li Z, Feng D, Xiong F, Liu J, Li J, Wang M, Wang J, Liu B, Wang H (2014) OsCERK 1 and
567 OsRLCK 176 play important roles in peptidoglycan and chitin signaling in rice innate
568 immunity. The Plant Journal 80: 1072–1084

569 Böhm H, Albert I, Oome S, Raaymakers TM, Van Den Ackerveken G, Nürnberger T (2014) A
570 conserved peptide pattern from a widespread microbial virulence factor triggers pattern-
571 induced immunity in Arabidopsis. PLoS Pathog 10: e1004491

572 Boller T, Felix G (2009) A renaissance of elicitors: Perception of microbe-associated molecular
573 patterns and danger signals by pattern-recognition receptors. Annu Rev Plant Biol 60: 379–
574 406

575 Brandizzi F, Irons SL, Johansen J, Kotzer A, Neumann U (2004) GFP is the way to glow: bioimaging
576 of the plant endomembrane system. Journal of Microscopy 214: 138–158

577 Brulé D, Villano C, Davies LJ, Trdá L, Claverie J, Héloir M, Chiltz A, Adrian M, Darblade B,
578 Tornero P, et al (2019) The grapevine (*Vitis vinifera*) LysM receptor kinases Vv LYK 1-1 and
579 Vv LYK 1-2 mediate chitooligosaccharide-triggered immunity. Plant Biotechnology Journal
580 17: 812–825

581 Buendia L, Wang T, Girardin A, Lefebvre B (2016) The LysM receptor-like kinase SlLYK10
582 regulates the arbuscular mycorrhizal symbiosis in tomato. New Phytologist 210: 184–195

583 Buendia L, Girardin A, Wang T, Cottret L, Lefebvre B (2018) LysM Receptor-Like Kinase and
584 LysM Receptor-Like Protein families: An update on phylogeny and functional
585 characterization. Front Plant Sci 9: 1531

586 Cao Y, Liang Y, Tanaka K, Nguyen CT, Jedrzejczak RP, Joachimiak A, Stacey G (2014) The kinase
587 LYK5 is a major chitin receptor in Arabidopsis and forms a chitin-induced complex with
588 related kinase CERK1. eLife 3: e03766

589 Claverie J, Balacey S, Lemaître-Guillier C, Brulé D, Chiltz A, Granet L, Noirot E, Daire X, Darblade
590 B, Héloir M-C, et al (2018) The cell wall-derived xyloglucan is a new DAMP triggering plant
591 immunity in *Vitis vinifera* and *Arabidopsis thaliana*. Front Plant Sci 9: 1725

592 Clough SJ, Bent AF (1998) Floral dip: a simplified method for *Agrobacterium*-mediated
593 transformation of *Arabidopsis thaliana*. The Plant Journal 16: 735–743

594 Cullimore J, Fliegmann J, Gasciolli V, Gibelin-Viala C, Carles N, Luu T-B, Girardin A, Cumener M,
595 Maillet F, Pradeau S, et al. (2023) Evolution of lipochitooligosaccharide binding to a LysM-RLK for
596 nodulation in *Medicago truncatula*. Plant And Cell Physiology 64: 746–757.

597 Ding Y, Wang T, Gasciolli V, Reyt G, Remblière C, Marcel F, François T, Bendahmane A, He G,
598 Bono JJ, et al (2024) The LysM Receptor-Like Kinase SlLYK10 controls
599 lipochitooligosaccharide signaling in inner cell layers of tomato roots. Plant and Cell
600 Physiology 65: 1149–1159

601 Ding Y, Lesterps Z, Gasciolli V, Fuchs AL, Gaston M, Medioni L, de-Regibus A, Remblière C,
602 Vicédo C. Bensmihen S et al (2025) Several groups of LysM-RLKs are involved in symbiotic
603 signal perception and arbuscular mycorrhiza establishment. Nat Commun 16: 5999

604 Feechan A, Anderson C, Torregrosa L, Jermakow A, Mestre P, Wiedemann-Merdinoglu S,
605 Merdinoglu D, Walker AR, Cadle-Davidson L, Reisch B, et al (2013) Genetic dissection of a
606 TIR-NB-LRR locus from the wild North American grapevine species *Muscadinia*
607 *rotundifolia* identifies paralogous genes conferring resistance to major fungal and oomycete
608 pathogens in cultivated grapevine. The Plant Journal 76: 661–674

609 Feng F, Sun J, Radhakrishnan GV, Lee T, Bozsóki Z, Fort S, Gavrin A, Gysel K, Thygesen MB,
610 Andersen KR, et al (2019) A combination of chitooligosaccharide and
611 lipochitooligosaccharide recognition promotes arbuscular mycorrhizal associations in
612 Medicago truncatula. Nat Commun 10: 5047

613 Fillinger S, Elad Y, eds (2016) Botrytis – the Fungus, the Pathogen and its Management in
614 Agricultural Systems. doi: 10.1007/978-3-319-23371-0

615 Gabler FM, Smilanick JL, Mansour M, Ramming DW, Mackey BE (2003) Correlations of
616 morphological, anatomical, and chemical features of grape berries with resistance to *Botrytis*
617 *cinerea*. Phytopathology® 93: 1263–1273

618 Gimenez-Ibanez S, Hann DR, Ntoukakis V, Petutschnig E, Lipka V, Rathjen JP (2009) AvrPtoB
619 targets the LysM Receptor Kinase CERK1 to promote bacterial virulence on plants. Current
620 Biology 19: 423–429

621 Girardin A, Wang T, Ding Y, Keller J, Buendia L, Gaston M, Ribeyre C, Gasciolli V, Auriac M-C,
622 Vernié T, et al (2019) LCO receptors involved in arbuscular mycorrhiza are functional for
623 rhizobia perception in legumes. Current Biology 29: 4249-4259.e5

624 Haile ZM, Malacarne G, Pilati S, Sonego P, Moretto M, Masuero D, Vrhovsek U, Engelen K, Baraldi
625 E, Moser C (2020) Dual transcriptome and metabolic analysis of *Vitis vinifera* cv. Pinot Noir
626 berry and *Botrytis cinerea* during quiescence and egressed infection. Front Plant Sci 10: 1704

627 Halter T, Imkampe J, Mazzotta S, Wierzba M, Postel S, Bücherl C, Kiefer C, Stahl M, Chinchilla D,
628 Wang X, et al (2014) The Leucine-Rich Repeat Receptor Kinase BIR2 is a negative regulator
629 of BAK1 in plant immunity. Current Biology 24: 134–143

630 Hanks SK, Quinn AM, Hunter T (1988) The protein kinase family: Conserved features and deduced
631 phylogeny of the catalytic domains. Science 241: 42–52

632 Hayafune M, Berisio R, Marchetti R, Silipo A, Kayama M, Desaki Y, Arima S, Squeglia F, Ruggiero
633 A, Tokuyasu K, et al (2014) Chitin-induced activation of immune signaling by the rice
634 receptor CEBiP relies on a unique sandwich-type dimerization. Proc Natl Acad Sci USA. doi:
635 10.1073/pnas.1312099111

636 He J, Zhang C, Dai H, Liu H, Zhang X, Yang J, Chen X, Zhu Y, Wang D, Qi X, et al (2019) A LysM
637 receptor heteromer mediates perception of arbuscular mycorrhizal symbiotic signal in rice.
638 Molecular Plant 12: 1561–1576

639 Jones DT, Taylor WR, Thornton JM (1992) The rapid generation of mutation data matrices from
640 protein sequences. Bioinformatics 8: 275–282

641 Karimi M, De Meyer B, Hilson P (2005) Modular cloning in plant cells. Trends in Plant Science 10:
642 103–105

643 Kelloniemi J, Trouvelot S, Héloir M-C, Simon A, Dalmais B, Frettinger P, Cimerman A, Fermaud
644 M, Roudet J, Baulande S, et al (2015) Analysis of the molecular dialogue between gray mold
645 (*Botrytis cinerea*) and grapevine (*Vitis vinifera*) reveals a clear shift in defense mechanisms
646 during berry ripening. MPMI 28: 1167–1180

647 Klaus-Heisen D, Nurisso A, Pietraszewska-Bogiel A, Mbengue M, Camut S, Timmers T, Pichereaux
648 C, Rossignol M, Gadella TWJ, Imberty A, et al (2011) Structure-function similarities between
649 a Plant Receptor-like Kinase and the Human Interleukin-1 Receptor-associated Kinase-4.
650 Journal of Biological Chemistry 286: 11202–11210

651 Kumar S, Stecher G, Li M, Knyaz C, Tamura K (2018) MEGA X: Molecular Evolutionary Genetics
652 Analysis across computing platforms. Molecular Biology and Evolution 35: 1547–1549

653 Li X-R, Sun J, Albinsky D, Zarrabian D, Hull R, Lee T, Jarratt-Barnham E, Chiu CH, Jacobsen A,
654 Soumpourou E, et al (2022) Nutrient regulation of lipochitooligosaccharide recognition in
655 plants via NSP1 and NSP2. Nat Commun 13: 6421

656 Liu H, Naismith JH (2008) An efficient one-step site-directed deletion, insertion, single and multiple-
657 site plasmid mutagenesis protocol. BMC Biotechnol 8: 91

658 Liu T, Liu Z, Song C, Hu Y, Han Z, She J, Fan F, Wang J, Jin C, Chang J, et al (2012) Chitin-
659 induced dimerization activates a plant immune receptor. Science 336: 1160–1164

660 Lovato A, Zenoni S, Tornielli GB, Colombo T, Vandelle E, Polverari A (2019) Plant and fungus
661 transcriptomic data from grapevine berries undergoing artificially-induced noble rot caused
662 by Botrytis cinerea. Data in Brief 25: 104150

663 Mason KN, Ekanayake G, Heese A (2020) Staining and automated image quantification of callose in
664 Arabidopsis cotyledons and leaves. Methods in Cell Biology. Elsevier, pp 181–199

665 Miya A, Albert P, Shinya T, Desaki Y, Ichimura K, Shirasu K, Narusaka Y, Kawakami N, Kaku H,
666 Shibuya N (2007) CERK1, a LysM receptor kinase, is essential for chitin elicitor signaling in
667 *Arabidopsis*. Proc Natl Acad Sci USA 104: 19613–19618

668 Morales J, Kadota Y, Zipfel C, Molina A, Torres M-A (2016) The Arabidopsis NADPH oxidases

669 *RbohD* and *RbohF* display differential expression patterns and contributions during plant
670 immunity. Journal of Experimental Botany 67: 1663–1676

671 Ngou BPM, Heal R, Wyler M, Schmid MW, Jones JDG (2022) Concerted expansion and contraction
672 of immune receptor gene repertoires in plant genomes. Nat Plants 8: 1146–1152

673 Pathak VM, Verma VK, Rawat BS, Kaur B, Babu N, Sharma A, Dewali S, Yadav M, Kumari R,
674 Singh S, et al (2022) Current status of pesticide effects on environment, human health and it's
675 eco-friendly management as bioremediation: A comprehensive review. Front Microbiol 13:
676 962619

677 Qiu W, Feechan A, Dry I (2015) Current understanding of grapevine defense mechanisms against the
678 biotrophic fungus (Erysiphe necator), the causal agent of powdery mildew disease. Hortic Res
679 2: 15020

680 Roudaire T, Marzari T, Landry D, Löffelhardt B, Gust AA, Jermakow A, Dry I, Winckler P, Héloir
681 M-C, Poinssot B (2023) The grapevine LysM receptor-like kinase VvLYK5-1 recognizes
682 chitin oligomers through its association with VvLYK1-1. Front Plant Sci 14: 1130782

683 Ruijter JM, Ramakers C, Hoogaars WMH, Karlen Y, Bakker O, Van Den Hoff MJB, Moorman AFM
684 (2009) Amplification efficiency: linking baseline and bias in the analysis of quantitative PCR
685 data. Nucleic Acids Research 37: e45–e45

686 Shimada TL, Shimada T, Hara-Nishimura I (2010) A rapid and non-destructive screenable marker,
687 FAST, for identifying transformed seeds of *Arabidopsis thaliana*. The Plant Journal, 61: 519-
688 528.

689 Shimizu T, Nakano T, Takamizawa D, Desaki Y, Ishii-Minami N, Nishizawa Y, Minami E, Okada
690 K, Yamane H, Kaku H, et al (2010) Two LysM receptor molecules, CEBiP and OsCERK1,
691 cooperatively regulate chitin elicitor signaling in rice: LysM receptors for rice chitin
692 signaling. The Plant Journal 64: 204–214

693 Silva CJ, Van Den Abeele C, Ortega-Salazar I, Papin V, Adaskaveg JA, Wang D, Casteel CL,
694 Seymour GB, Blanco-Ulate B (2021) Host susceptibility factors render ripe tomato fruit
695 vulnerable to fungal disease despite active immune responses. Journal of Experimental
696 Botany 72: 2696–2709

697 Spoel SH, Koornneef A, Claessens SMC, Korzelius JP, Van Pelt JA, Mueller MJ, Buchala AJ,
698 Métraux J-P, Brown R, Kazan K, et al (2003) NPR1 modulates cross-talk between Salicylate-
699 and Jasmonate-Dependent defense pathways through a novel function in the cytosol. Plant
700 Cell 15: 760–770

701 Trdá L, Fernandez O, Boutrot F, Héloir M, Kelloniemi J, Daire X, Adrian M, Clément C, Zipfel C,
702 Dorey S, et al (2014) The grapevine flagellin receptor VvFLS2 differentially recognizes
703 flagellin-derived epitopes from the endophytic growth-promoting bacterium *Burkholderia*
704 *phytofirmans* and plant pathogenic bacteria. New Phytologist 201: 1371–1384

705 Vetter MM, Kronholm I, He F, Haweker H, Reymond M, Bergelson J, Robatzek S, De Meaux J
706 (2012) Flagellin perception varies quantitatively in *Arabidopsis thalia*na and its relatives.
707 Molecular Biology and Evolution 29: 1655–1667

708 Wan J, Tanaka K, Zhang X-C, Son GH, Brechenmacher L, Nguyen THN, Stacey G (2012) LYK4, a
709 Lysin Motif Receptor-Like Kinase, is important for chitin signaling and plant innate
710 immunity in Arabidopsis. Plant Physiology 160: 396–406

711 Wang T, Gasciolli V, Gaston M, Medioni L, Cumener M, Buendia L, Yang B, Bono JJ, He G,
712 Lefebvre B (2023) LysM receptor-like kinases involved in immunity perceive lipo-
713 chitooligosaccharides in mycotrophic plants. Plant Physiology 192: 1435–1448

714 Xiao H, Liu Z, Wang N, Long Q, Cao S, Huang G, Liu W, Peng Y, Riaz S, Walker AM, et al (2023)
715 Adaptive and maladaptive introgression in grapevine domestication. Proc Natl Acad Sci USA
716 120: e2222041120

717 Xu L, Wang J, Xiao Y, Han Z, Chai J (2023) Structural insight into chitin perception by chitin
718 elicitor receptor kinase 1 of *Oryza sativa*. JIPB 65: 235–248

719 Xue D-X, Li C-L, Xie Z-P, Staehelin C (2019) LYK4 is a component of a tripartite chitin receptor
720 complex in *Arabidopsis thaliana*. Journal of Experimental Botany 70: 5507–5516

721 Zaidi SS-A, Mukhtar MS, Mansoor S (2018) Genome Editing: Targeting Susceptibility Genes for
722 Plant Disease Resistance. Trends in Biotechnology 36: 898–906

723 Zhang C, He J, Dai H, Wang G, Zhang X, Wang C, Shi J, Chen X, Wang D, Wang E (2021)
724 Discriminating symbiosis and immunity signals by receptor competition in rice. Proc Natl
725 Acad Sci USA 118: e2023738118

726 Zhou J-M, Zhang Y (2020) Plant immunity: Danger perception and signaling. Cell 181: 978–989

727 Zimmerli L, Métraux J-P, Mauch-Mani B. (2001) β-Aminobutyric acid-induced protection of
728 Arabidopsis against the necrotrophic fungus *Botrytis cinerea*. *Plant Physiology* 126: 517–523.

729 Zipfel C (2014) Plant pattern-recognition receptors. Trends in Immunology 35: 345–351

730 Zouine M, Maza E, Djari A, Lauvernier M, Frasse P, Smouni A, Pirrello J, Bouzayen M. (2017)
731 TomExpress, a unified tomato RNA-Seq platform for visualization of expression data, clustering and
732 correlation networks. *The Plant Journal* 92: 727–735.

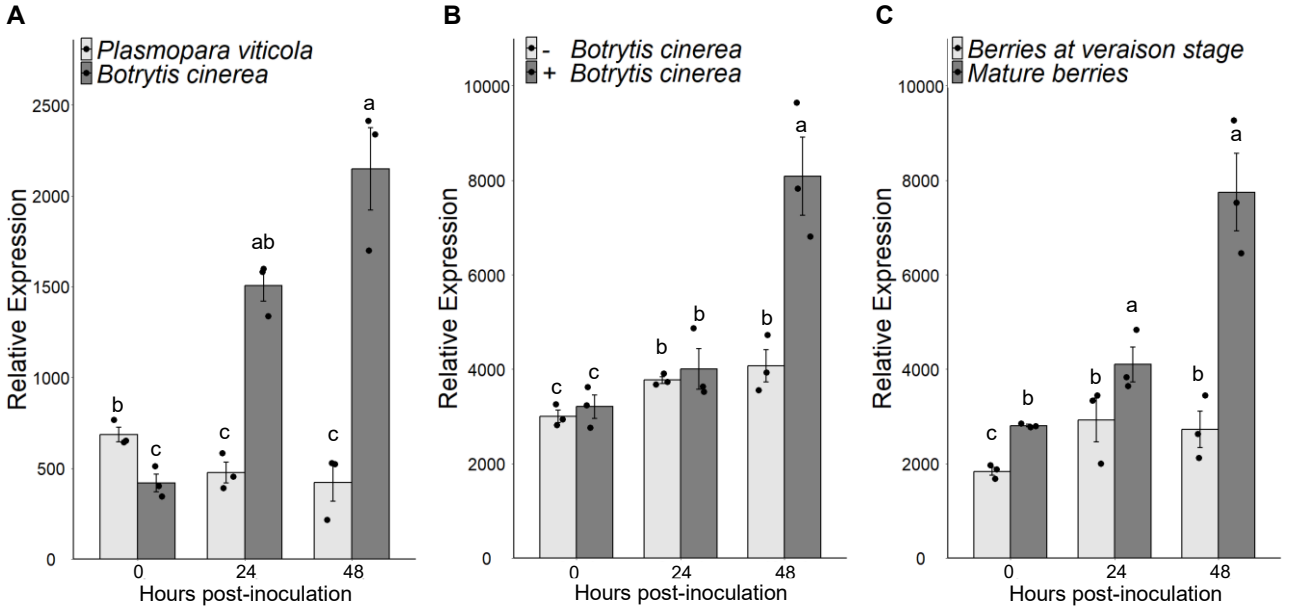

Figure 1. *VvLYK6* is induced during *Botrytis cinerea* infection on grapevine leaves and mature berries. (A) *VvLYK6* expression profiles analyzed at 0, 24 and 48 h post-inoculation on leaves infected either by *Botrytis cinerea* or *Plasmopara viticola*. **(B)** *VvLYK6* expression profiles analyzed at 0, 24 and 48 h post-inoculation on ripe berries infected or not with *B. cinerea*. **(C)** Comparison of *VvLYK6* expression on grapevine berries infected with *B. cinerea* at two stages of grapevine development corresponding to berries at veraison stage and ripe berries, respectively. For each bar plot, bars represent the mean ± SEM on three biologically independent experiments and statistically significant groups are categorized by different letters (Kruskal-Wallis/BH post-test; P<0.05). All transcriptomic data were generated from Kelloniemi et al. (2015).

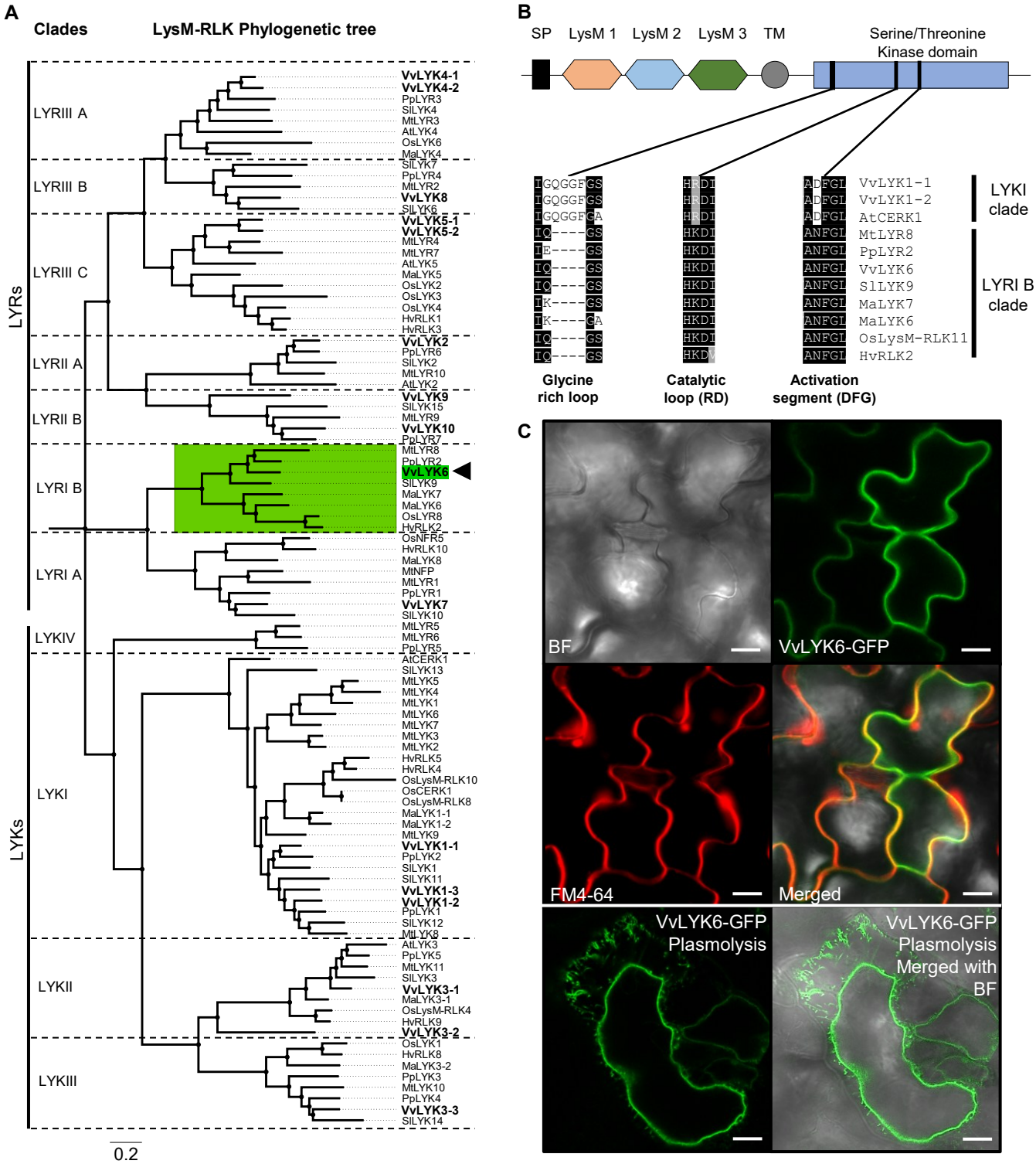

Figure 2. *VvLYK6* belongs to the LYRI B phylogenetic clade of the LysM receptor-like kinases family. (A) A 1000 bootstrapped Maximum-likelihood phylogenetic tree (Jones-Taylor-Thornton (JTT) model) with LysM-RLKs from 8 plant species was constructed with MEGA X (Kumar *et al.*, 2018). Phylogenetic tree was subdivided by clades according to the phylogenetic analysis from Buendia *et al.* (2018). LYKs correspond to LysM-RLKs with an active kinase domain and LYRs correspond to LYK-related LysM-RLKs without kinase activity. Protein sequences are listed in supplemental Table S1. The 16 LysM-RLKs found in grapevine genome (VvLYKs) are in bold. VvLYK6 is highlighted in green and indicated by a black arrow inside the green-surrounded LYRI B clade. **(B)** Schematic representation of putative VvLYK6 domains. Black square: Signal peptide, hexagon: LysM domain, LysM1 (orange), LysM2 (blue), LysM3 (green), grey circle: transmembrane domain and blue square: kinase domain. Below schematic VvLYK6 structure are shown alignments of motifs involved in kinase activity (Glycine rich-loop, Catalytic loop (RD) and activation segment (DFG motif). Protein domain sequences were aligned with Clustal performed on MEGAX (Kumar *et al.*, 2018). Black and grey shading representing conservation of amino acids. The alignment includes VvLYK1-1, VvLYK1-2, AtCERK1 belonging to the LYKI clade and MtLYR8, PpLYR2, VvLYK6, SlLYK9, MaLYK7, MaLYK6, OsLysM-RLK11/OsLYR8 and HvRLK2 belonging to the LYRI B clade. **(C)** Subcellular localization of VvLYK6 in *A. thaliana* leaves. GFP-tagged VvLYK6 in leaf segments of *A. thaliana* co-localizes with the plasma membrane marker probe (FM4-64). Plasmolysis of plant cells expressing VvLYK6 tagged with GFP reveals that the GFP signal does not localize to the cell wall. Scale bars represent 20 µm. Similar localization was observed in three independent lines. BF = Brightfield.

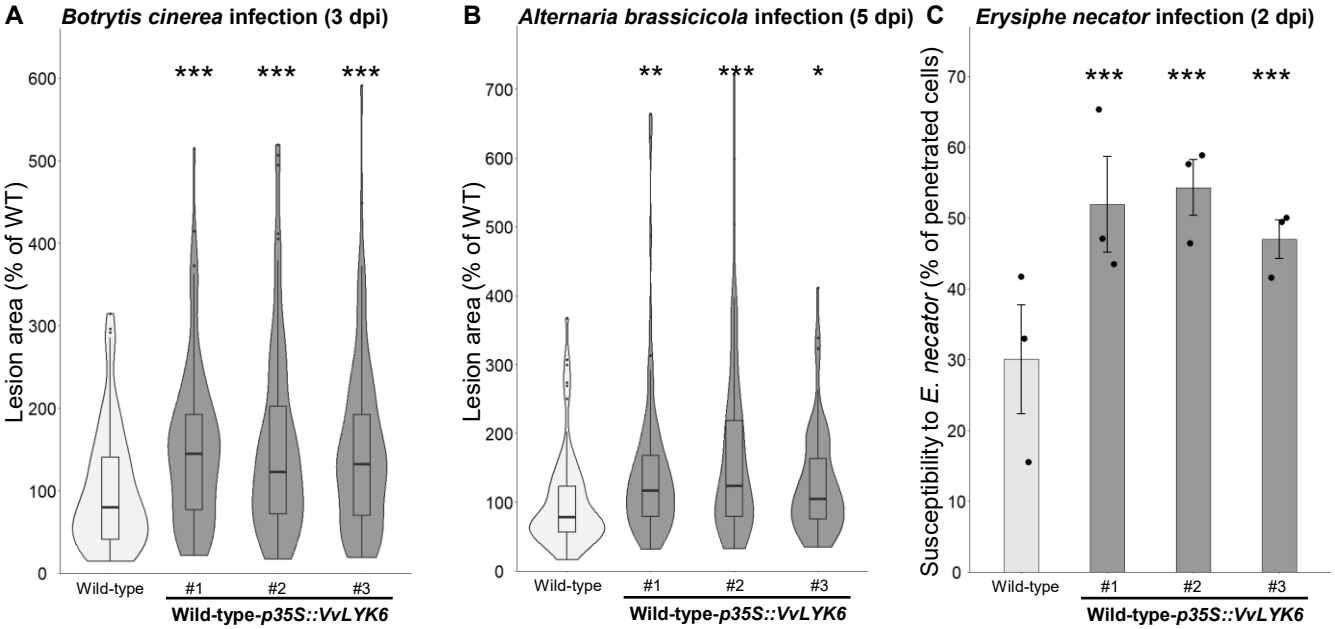

Figure 3. Constitutive expression of *VvLYK6* in *A. thaliana* increases its susceptibility to different fungal pathogens. (A) Disease lesions percentage induced by *B. cinerea* on Wild-type (WT) and the three independent transgenic lines expressing *VvLYK6* measured 3 days post inoculation, lesion area on WT plants are referred as 100%. Violin plot with included boxplot illustrates the distribution of lesions percentage of three independent experiments. For each biological replicate, 32 lesions were scored from 8 plants per line, combining data from 3 biological replicates. Each transgenic line was statistically compared to the WT with the non-parametric Wilcoxon test (***, P<0.001). **(B)** Lesions percentage provoked by the necrotrophic fungus *A. brassicicola* on the WT and the three independent transgenic lines constitutively expressing *VvLYK6,* measured five days post inoculation. Violin plot with included boxplot represents distribution of lesions percentage of five independent experiments. For each biological replicate, 18 lesions were scored from four plants per line, combining data from 4 biological replicates. Each transgenic line was statistically compared to the WT with the non-parametric Wilcoxon test (***, P<0.001; **, P<0.01; *, P<0.05). **(C)** Penetration of the non-adapted powdery mildew *E. necator* on the WT and the three independent transgenic lines constitutively expressing *VvLYK6* measured 2 days post inoculation. Bars represent the mean percentage of epidermal penetrated cells from three biologically independent experiments each with more than one hundred germinated conidia counted ± SEM. Each transgenic line was statistically compared to the WT with a pairwise comparison of proportions test (***, P<0.001).

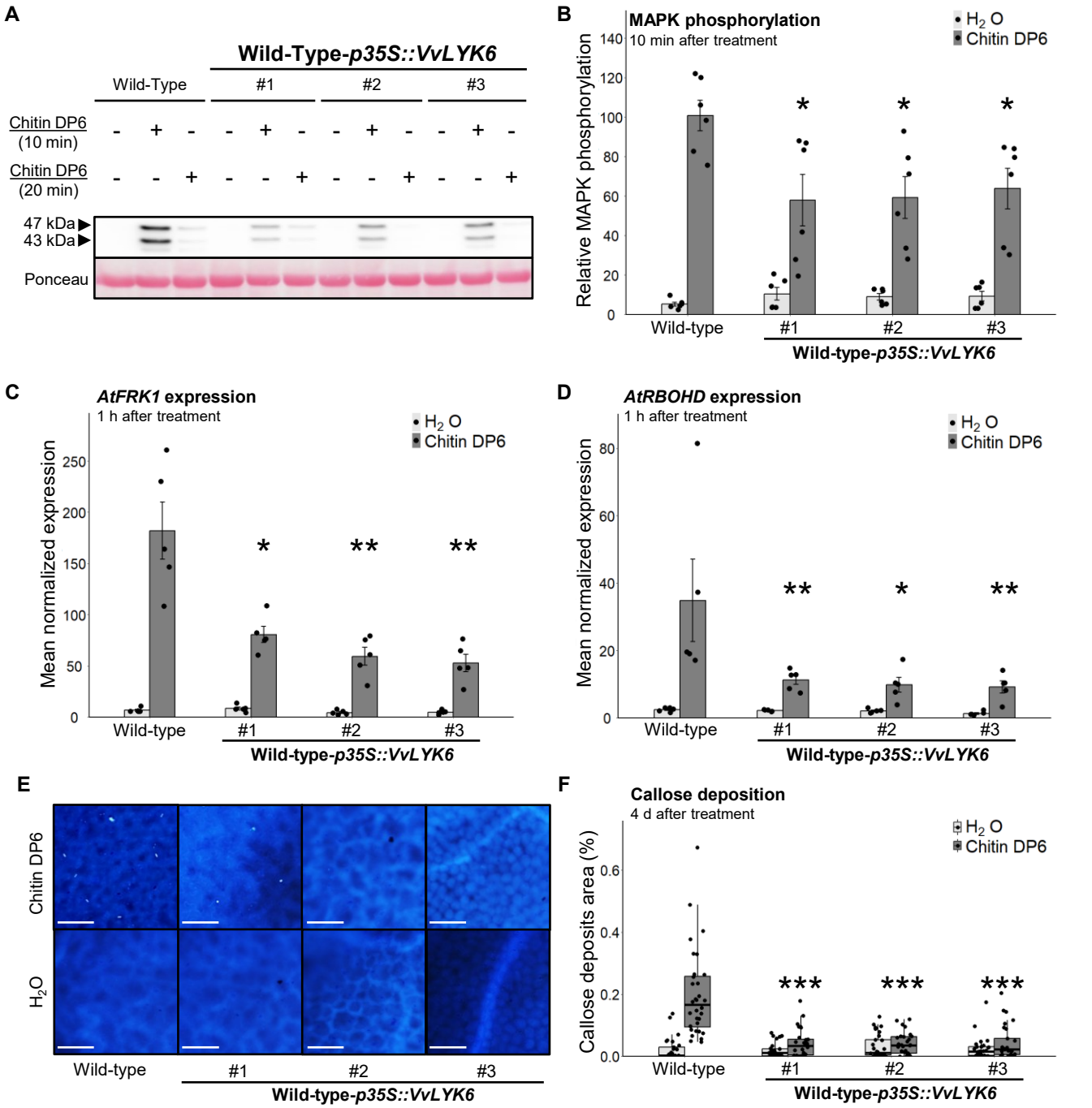

Figure 4. Constitutive expression of VvLYK6 inhibits chitin-triggered immune responses in *A. thaliana*. (A-B) MAPKs phosphorylation was detected 10 min or 20 min after H_2O (-) or chitin DP6 treatment (0.05 g/L) by immunoblotting with an antibody α-pERK1/2 in the Wild-Type (WT) and three independent lines constitutively expressing *VvLYK6*. (a) Representative immunoblotting with α-pERK1/2 and homogeneous loading verified by Ponceau red staining. **(B)** Quantification of the MAPKs phosphorylation at 10 min after treatment, detected by ImageQuant. Bars represent the mean ± SEM on 6 biologically independent experiments. Each *VvLYK6*-expressing line treated with chitin DP6 was statistically compared to the WT with the non-parametric Wilcoxon test (*, P<0.05). **(C-D)** Normalized expression level of *AtFRK1* and *AtRBOHD* measured by qPCR 1h after chitin DP6 (0.05 g/L) or H_2O treatment. The expression levels of *AtFRK1* and *AtRBOHD* were normalized to those of two housekeeping genes. Bars represent the mean of relative expression ± SEM of 5 biologically independent experiments. Asterisks indicate a statistically significant difference between each transgenic line and the WT treated with chitin DP6, (non-parametric Wilcoxon test; *, P<0.05; **, P<0.01). **(E)** Representative pictures of callose deposition after chitin DP6 (0.05g/L) or H_2O treatment in WT or the three *VvLYK6*-expressing lines, observed 4 days post-treatment and analyzed by epifluorescence microscopy after aniline blue staining. Callose deposits were quantified with Trainable Weka Segmentation plugin in imageJ. **(F)** Box plot represents distribution of callose deposits percentage on total leaves surface for each genotype and condition on at least 30 pictures per condition from three biologically independent experiments. Asterisks indicate a significant difference between each line expressing *VvLYK6* and WT treated with DP6 (Wilcoxon test, ***; P<0.001).

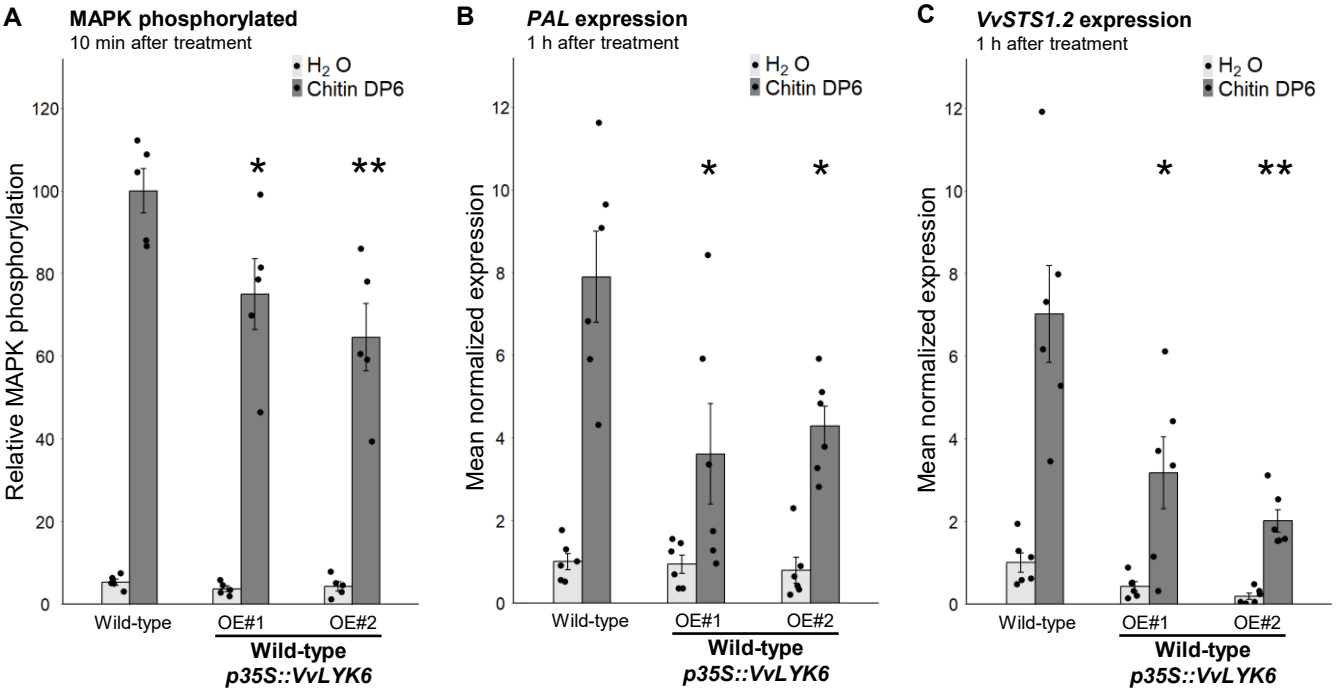

Figure 5. VvLYK6 is also a repressor of chitin-triggered immune responses in *V. vinifera*. (A) Quantification of the MAPKs phosphorylation detected 10 min after H_2O or DP6 treatment (0.05 g/L) by immunoblotting with an antibody α-pERK1/2 in the WT grapevine cell line and two independent lines constitutively expressing VvLYK6-GFP. MAPKs phosphorylation was quantified by ImageQuant. Bars represent the mean ± SEM on five biologically independent experiments. Each *VvLYK6*-expressing cell line was statistically compared to the corresponding WT grapevine cells treated with DP6 using the non-parametric Wilcoxon test (*, P<0.05; **, P <0.01). **(B-C)** Normalized expression level of *VvPAL* **(B)** and V*vSTS1.2* **(C)** measured by qPCR 1h after DP6 (0.05 g/L) or H_2O treatment. The expression levels of *VvPAL and VvSTS1.2* were normalized to those of two housekeeping genes. Bars represent the mean of relative expression ± SEM of 6 biologically independent experiments. Asterisks indicate a statistically significant difference between each transgenic line and the WT treated with DP6 using a pairwise Wilcoxon test (*, P<0.05; **, P <0.01).

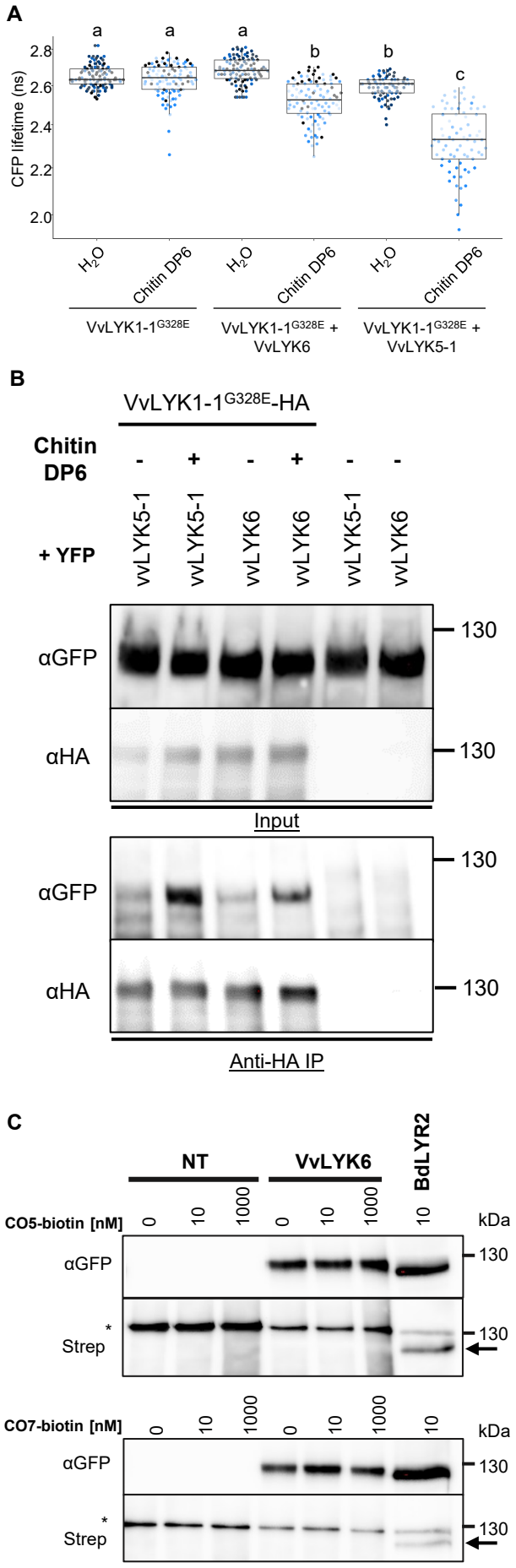

Figure 6. VvLYK6 interacts with VvLYK1-1 in presence of chitin oligomers. (A) The dead kinase VvLYK1-1^{G328E}-CFP was transiently expressed in *Nicotiana benthamiana* leaves alone or together with VvLYK6-YFP or VvLYK5-1-YFP, a protein known to interacts with VvLYK1-1 in presence of chitin DP6 (Roudaire *et al.*, 2023). CFP lifetime (ns) was measured after leaves treatment with either water (H_2O) or chitin DP6 (0,1 g/L). Boxplots represent the distribution of the data acquired in at least three biologically independent experiments. Different letters indicate a significant difference using a non-parametric Kruskal-Wallis test. **(B)** Co-immunopurification (Co-IP) of VvLYK1-1^{G328E}-HA with VvLYK5-1:YFP and VvLYK6:YFP in presence or not of chitin DP6. Extracted proteins from *N. benthamiana* leaves were purified using anti-HA beads (Anti-HA IP). After IP, corresponding proteins were detected with anti-GFP antibodies (αGFP) and anti-HA antibodies (αHA). **(C)** The LysM-RLK VvLYK6 alone is not able to bind CO5 or CO7 with high affinity. VvLYK6-YFP and BdLYR2-YFP were transiently expressed in *N. benthamiana* leaves. Subsequently, microsomal fractions were prepared, and binding assays were conducted using a range of CO5-biotin or CO7-biotin as ligand. Microsomal fractions from leaves expressing BdLYR2-YFP were used as positive control (black arrow) while those from non-transformed (NT) leaves served as negative control. Western blotting was conducted using αGFP and streptavidin-HRP. The quantities of microsomal fractions used correspond to 50 µg of total proteins for VvLYK6-YFP and NT, and 5 µg for BdLYR2-YFP. The asterisk represents an unspecific band (endogenously biotinylated protein) observed at 130 KDa. No binding with CO5-biotin or CO7-biotin were observed with VvLYK6.

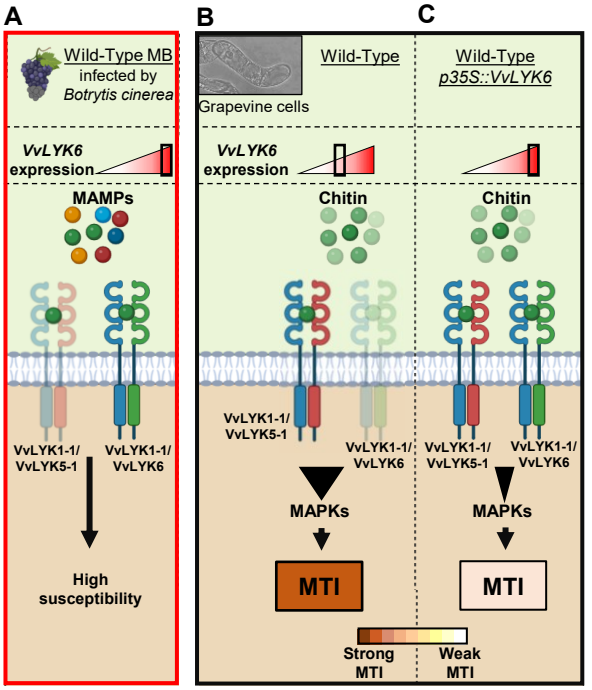

Figure 7. Proposed mode of action of VvLYK6 to modulate plant immune responses. VvLYK6 is involved in grapevine susceptibility during *Botrytis cinerea* infection and repression of chitin oligomer elicitation. **(A)** *VvLYK6* expression is induced during *Botrytis cinerea* infection in mature berries (MB), correlated with the absence of defense gene (*VvSTS1.2* and *VvPAL*) and a high susceptibility to fungal pathogens (Kelloniemi *et al.*, 2015). **(B)** Formation of a VvLYK1-1 / VvLYK5-1 complex after perception of chitin oligomers at the plasma membrane to activate a strong MAMP-triggered immunity (MTI) in grapevine cells (Roudaire *et al.*, 2023). **(C)** Constitutive expression of VvLYK6, which interacts with VvLYK1-1, might deplete VvLYK1-1 for its interaction with VvLYK5-1 and decrease chitin-triggered plant defense responses. Receptors have been classified by colour, VvLYK1-1 = blue, VvLYK5-1 = red, VvLYK6 = green.